Submitted to the
The 2009 Europhysics Conference on High Energy Physics
July 16 - 22, 2009, Cracow, Poland

Abstract: 254 **Session: Higgs and New Physics**

Search for contact interactions in $e^{\pm}p$ collisions with ZEUS experiment at HERA.

ZEUS Collaboration

Abstract

A search for physics beyond the Standard Model is performed with high-Q^2 neutral current deep inelastic scattering events recorded with the ZEUS detector at HERA. Complete data on scattering of polarized electrons and positrons from HERA II running are combined with electron and positron data from HERA I, resulting in a total luminosity of $0.44\,\mathrm{fb}^{-1}$. No significant deviations from the Standard Model predictions are observed. Limits are derived on the effective mass scale in *eeqq* contact interactions, on the mass to the Yukawa coupling ratio for heavy-leptoquark models, on the effective Planck-mass scale in models with large extra dimensions and on the quark charge radius.

1 Introduction

Measurements of the deep inelastic $e^{\pm}p$ scattering (DIS) in the domain of very high values of Q^2, $Q^2 \sim 10^4\,\text{GeV}^2$ allow searches for new physics processes with characteristic mass scales in the TeV range. New interactions between electrons and quarks involving mass scales above the center-of-mass energy can modify the cross section at high Q^2 via virtual effects, resulting in observable deviations from the Standard Model (SM) predictions. Many such interactions, such as processes mediated by heavy leptoquarks, can be modelled as four-fermion contact interactions.

In the analysis of 1994-2000 $e^{\pm}p$ data [1], the ZEUS Collaboration applied a common method to search for four-fermion interactions, for graviton exchange in models with large extra dimensions, and for a finite charge radius of the quark. Results presented in this contribution extend the previous analysis [1] to include also the data collected with the ZEUS detector in 2003-2007, after the upgrade of the HERA accelerator.

2 Data and analysis method

The data used in this analysis were collected with the ZEUS detector at HERA and correspond to an integrated luminosity of $128\,\text{pb}^{-1}$ for $e^{\pm}p$ collisions collected in 1994-2000 (HERA I data) and $307\,\text{pb}^{-1}$ for $e^{\pm}p$ collisions collected in 2003-2007 (HERA II). The 1994-97 data set was collected at $\sqrt{s} = 300\,\text{GeV}$ and the 1998-2007 data sets were taken with $\sqrt{s} = 318\,\text{GeV}$. In 2003-2007 HERA was running with longitudinally polarized beam: for electron data sets the mean luminosity-weighted polarization was -0.27 and $+0.29$, whereas for positron data the mean polarization of -0.37 and $+0.32$ was obtained. Data samples taken with opposite electron or positron polarizations were considered separately, to increase the sensitivity of the search.

This study exploits the event samples from the previously published HERA I and HERA II $e^{\pm}p$ cross section measurements [2–6] and from the preliminary HERA II $e^{+}p$ analysis [7]. The CI analysis compares the measured distribution of the kinematic variable Q^2, in each of the considered data samples, with the predictions of the Monte Carlo (MC) simulation. The effects of each CI scenario are taken into account by appropriately reweighting the Standard Model (SM) MC. This approach guarantees that possible differences between the SM and the CI model in event-selection efficiency and migration corrections are properly taken into account. To minimize the influence of normalization uncertainties, model predictions are always normalized to the corresponding data sample, so only the shapes of the distributions are compared. For each data sample the likelihood function is determined from the measured Q^2 distribution, using Poissonian statistics for the event numbers in

Q^2 intervals. The likelihood for the complete $e^{\pm}p$ data set is obtained by multiplying the likelihoods for each of the considered data samples. Only events with $Q^2 > 560\,\mathrm{GeV}^2$ are used in the analysis.

The limit-setting method is based on the comparison of the most likely model coupling strength (determined from the likelihood maximum) for the collected ZEUS data and for a large number of equivalent MC experiments. Excluded at the 95% C.L. are models which, in more than 95% of the MC experiments, result in a most likely coupling strength greater than the one determined for the actual data. For the preliminary results presented here, the following systematic uncertainties have been included in the generation of the MC experiments: electron energy-scale uncertainty, hadron energy-scale uncertainty, uncertainties in the parton density functions (PDF) resulting from the uncertainty in the value of $\alpha_S(M_Z^2)$ used in the NLO QCD fit and from the statistical and systematic uncertainties of the input data, as given by the ZEUS-S fit [8]. Details of the methods used to set parameter limits are described in [1].

3 Models for new physics

3.1 General contact interactions

Four-fermion contact interactions (CI) represent an effective theory which describes low-energy effects due to physics at much higher energy scales. CI models describe the effects of heavy leptoquarks, additional heavy weak bosons and electron or quark compositeness. The CI approach is not renormalizable and is only valid in the low-energy limit. As strong limits have already been placed on scalar and tensor contact interactions [9], only vector currents are considered here. They can be represented by additional terms in the Standard Model Lagrangian, viz:

$$\mathcal{L}_{CI} = \sum_{\substack{i,j=L,R \\ q=u,d,s,c,b}} \eta_{ij}^{eq} (\bar{e}_i \gamma^{\mu} e_i)(\bar{q}_j \gamma_{\mu} q_j) \, , \qquad (1)$$

where the sum runs over electron and quark helicities and quark flavors. The couplings η_{ij}^{eq} describe the helicity and flavor structure of contact interactions. It was assumed that all up-type quarks have the same contact-interaction couplings, and a similar assumption was made for down-type quarks:

$$\begin{aligned} \eta_{ij}^{eu} &= \eta_{ij}^{ec} &= \eta_{ij}^{et} \, , \\ \eta_{ij}^{ed} &= \eta_{ij}^{es} &= \eta_{ij}^{eb} \, , \end{aligned}$$

leading to eight independent couplings, η_{ij}^{eq}, with $q = u, d$. Due to the impracticality of setting limits in an eight-dimensional space, a set of representative scenarios was analyzed.

Each scenario is defined by a set of eight coefficients, ϵ_{ij}^{eq}, each of which may take the values ± 1 or zero, and the compositeness scale Λ. The couplings are then defined by

$$\eta_{ij}^{eq} = \epsilon_{ij}^{eq} \frac{4\pi}{\Lambda^2} .$$

Note that models that differ in the overall sign of the coefficients ϵ_{ij}^{eq} are distinct because of the interference with the SM.

3.2 Leptoquarks

Leptoquarks (LQ) appear in certain extensions of the SM that connect leptons and quarks; they carry both lepton and baryon numbers and have spin 0 or 1. According to the general classification proposed by Buchmüller, Rückl and Wyler [10], there are 14 possible LQ states: seven scalar and seven vector[1]. In the limit of heavy LQs ($M_{LQ} \gg \sqrt{s}$), the effect of s- and t-channel LQ exchange is equivalent to a vector-type $eeqq$ contact interaction[2]. The effective contact-interaction couplings, η_{ij}^{eq}, are proportional to the square of the ratio of the leptoquark Yukawa coupling, λ_{LQ}, to the leptoquark mass, M_{LQ}:

$$\eta_{ij}^{eq} = a_{ij}^{eq} \left(\frac{\lambda_{LQ}}{M_{LQ}} \right)^2 ,$$

where the coefficients a_{ij}^{eq} depend on the LQ species [12] and are twice as large for vector as for scalar leptoquarks. Only first-generation leptoquarks are considered in this analysis, $q = u, d$.

3.3 Large extra dimensions

Arkani-Hamed, Dimopoulos and Dvali [13–15] have proposed a model to solve the hierarchy problem, assuming that space-time has $4 + n$ dimensions. Particles, including strong and electroweak bosons, are confined to four dimensions, but gravity can propagate into the extra dimensions. The extra n spatial dimensions are compactified with a radius R. The Planck scale, $M_P \sim 10^{19}$ GeV, in 4 dimensions is an effective scale arising from the fundamental Planck scale M_D in $D = 4 + n$ dimensions. At high energies, the strengths of the gravitational and electroweak interactions can then become comparable. After summing the effects of graviton excitations in the extra dimensions, the graviton-exchange

[1] Leptoquark states are named according to the so-called Aachen notation [11].

[2] For the invariant mass range accessible at HERA, $\sqrt{s} \sim 300$ GeV, heavy LQ approximation is applicable for $M_{LQ} > 400$ GeV.

contribution to $eq \to eq$ scattering can be described as a contact interaction[3] with an effective coupling strength of [16, 17]

$$\eta_G = \frac{\lambda}{M_S^4},$$

where M_S is an ultraviolet cutoff scale, expected to be of the order of M_D, and the coupling λ is of order unity. Since the sign of λ is not known *a priori*, both values $\lambda = \pm 1$ are considered in this analysis. Graviton exchange also contributes to electron-gluon scattering, $eg \to eg$, which is not present at leading order in the SM.

3.4 Quark form factor

Quark substructure can be detected by measuring the spatial distribution of the quark charge. If $Q^2 \ll 1/R_e^2$ and $Q^2 \ll 1/R_q^2$, the SM predictions for the cross sections are modified, approximately, to:

$$\frac{d\sigma}{dQ^2} = \frac{d\sigma^{SM}}{dQ^2} \left(1 - \frac{R_e^2}{6} Q^2\right)^2 \left(1 - \frac{R_q^2}{6} Q^2\right)^2,$$

where R_e and R_q are the root-mean-square radii of the electroweak charge of the electron and the quark, respectively.

4 Results

The measured Q^2 spectra for e^+p and e^-p data, compared to the SM predictions using the CTEQ5D parameterization [18] of the proton PDF are shown in Fig. 1. No significant deviation of the ZEUS data from the SM prediction was observed. For all models considered, the best description of the data was obtained for very small values of model coupling strength, i.e. close to the SM. Therefore, limits on the strength parameters of the models described in Sec. 3 are presented in this paper. Systematic uncertainties are incorporated in the limit setting precedure, as described in Sec. 2.

Also shown in Fig. 1 are curves, for VV and AA contact-interaction models (Section 3.1), which correspond to the 95% C.L. exclusion limits on Λ. The 95% C.L. limits on the compositeness scale Λ, for different CI models, are compared in Fig. 2 and Table 1. Limits range from 3.8 TeV for the LR and VA models to 8.9 TeV for the VV model.

[3] Due to additional energy-scale dependence, reflecting the number of accessible graviton excitations, these contact interactions are not equivalent to the vector contact interactions of Eq. (1).

The leptoquark analysis takes into account LQs that couple to the electron and the first-generation quarks (u, d) only (Section 3.2). Deviations in the Q^2 distribution of e^+p and e^-p NC DIS events, corresponding to the 95% C.L. exclusion limits for selected scalar and vector leptoquark models, are compared with ZEUS data in Fig. 3. The 95% C.L. limits on the ratio of the leptoquark mass to the Yukawa coupling, M_{LQ}/λ_{LQ}, are summarized in Table 2 together with the coefficients a_{ij}^{eq} describing the CI coupling structure. The limits range from 0.41 TeV for $\tilde{S}_{\circ}^{R}$ model to 1.88 TeV for V_1^L model.

For the model with large extra dimensions (Section 3.3), 95% C.L. lower limits on the mass scale in n dimensions of

$$M_S \quad > \quad 0.94\,\mathrm{TeV}$$

were obtained for both coupling signs, $\lambda = \pm 1$. In Fig. 4, effects of graviton exchange on the Q^2 distribution, corresponding to these limits, are compared with ZEUS e^+p (Fig. 4a) and e^-p (Fig. 4b) data.

Assuming the electron to be point-like ($R_e = 0$), the 95% C.L. upper limit on the effective quark-charge radius (Section 3.4) of

$$R_q \quad < \quad 0.63 \cdot 10^{-16}\,\mathrm{cm}$$

was obtained. If the charge distribution in the quark changes sign as a function of the radius, negative values can also be considered for R_q^2. For such a model, the ZEUS 95% C.L. upper limit on the effective quark-charge radius squared can be written as:

$$-R_q^2 \quad < \quad (0.57 \cdot 10^{-16}\,\mathrm{cm})^2 \; .$$

Cross section deviations corresponding to the 95% C.L. exclusion limits for the effective radius, R_q, of the electroweak charge of the quark are compared with the ZEUS data in Fig. 4c.

5 Conclusions

A search for signatures of physics beyond the Standard Model has been performed with the e^+p and e^-p data collected with the ZEUS detector in the years 1994-2007. No significant deviation from Standard Model predictions was observed and 95% C.L. limits were obtained for the relevant parameters of the models studied. For the contact-interaction models, limits on the effective mass scale, Λ (i.e. compositeness scale), ranging from 3.8 to 8.9 TeV have been obtained. Limits ranging from 0.41 to 1.88 TeV have been set for the ratio of the leptoquark mass to the Yukawa coupling, M_{LQ}/λ_{LQ}, in the limit of large leptoquark masses, $M_{LQ} \gg \sqrt{s}$. Limits were derived on the mass scale parameter in models with large extra dimensions: scales below 0.94 TeV are excluded for both positive and negative coupling signs. A quark-charge radius larger than $0.63 \cdot 10^{-16}$ cm has been excluded, using the classical form-factor approximation.

References

[1] ZEUS Coll., S. Chekanov et al., Phys. Lett. **B 591**, 23 (2004).

[2] ZEUS Coll., J. Breitweg et al., Eur. Phys. J. **C 11**, 427 (1999).

[3] ZEUS Coll., S. Chekanov et al., Eur. Phys. J. **C 28**, 175 (2003).

[4] ZEUS Coll., S. Chekanov et al., Phys. Rev. **D 70**, 052001 (2004).

[5] ZEUS Coll., S. Chekanov et al., Phys. Lett. **B 637**, 210 (2006).

[6] ZEUS Coll., S. Chekanov et al., *Measurement of high-Q^2 neutral current deep inelastic e^-p scattering cross sections with a longitudinally polarised electron beam at HERA*. DESY-08-202 (2008), arXiv 0901.2385, accepted by EPJ C.

[7] ZEUS Coll., *Measurement of high-Q^2 neutral current deep inelastic e^+p scattering cross sections with longitudinally polarised electrons with ZEUS at HERA*. Submitted to XXXIV International Conference on High Energy Physics, Philadelphia, USA, 2008.

[8] ZEUS Coll., S. Chekanov et al., Phys. Rev. **D 67**, 012007 (2003).

[9] P. Haberl, F. Schrempp and H.U. Martyn, *Proc. Physics at HERA, vol. 2*, W. Buchmüller and G. Ingelman (eds.), p. 1133. Hamburg, Germany, DESY (1991).

[10] W. Buchmüller, R. Rückl and D. Wyler, Phys. Lett. **B 191**, 442 (1987). Erratum in Phys. Lett. **B 448**, 320 (1999).

[11] A. Djouadi et al., Z. Phys. **C 46**, 679 (1990).

[12] J. Kalinowski et al., Z. Phys. **C 74**, 595 (1997).

[13] N. Arkani-Hamed, S. Dimopoulos and G. Dvali, Phys. Lett. **B 429**, 263 (1998).

[14] I. Antoniadis, et al., Phys. Lett. **B436**, 257 (1998).

[15] N. Arkani-Hamed, S. Dimopoulos and G. Dvali, Phys. Rev. **D 59**, 086004 (1999).

[16] G.F. Giudice, R. Rattazzi and J.D. Wells, Nucl. Phys. **B 544**, 3 (1999).

[17] K. Cheung, Phys. Lett. **B460**, 383 (1999).

[18] CTEQ Coll., H.L. Lai et al., Eur. Phys. J. **C 12**, 375 (2000).

ZEUS 1994-2007 (prel.) $e^{\pm}p$			
	Coupling structure	95% C.L. (TeV)	
Model	$[\epsilon_{LL},\epsilon_{LR},\epsilon_{RL},\epsilon_{RR}]$	Λ^-	Λ^+
LL	$[+1, 0, 0, 0]$	4.0	5.2
LR	$[0, +1, 0, 0]$	3.8	5.2
RL	$[0, 0, +1, 0]$	4.2	4.9
RR	$[0, 0, 0, +1]$	4.6	4.6
VV	$[+1, +1, +1, +1]$	8.0	8.9
AA	$[+1, -1, -1, +1]$	7.0	6.7
VA	$[+1, -1, +1, -1]$	3.8	4.1
X1	$[+1, -1, 0, 0]$	5.1	5.0
X2	$[+1, 0, +1, 0]$	5.4	6.5
X3	$[+1, 0, 0, +1]$	6.2	6.8
X4	$[0, +1, +1, 0]$	6.0	6.9
X5	$[0, +1, 0, +1]$	5.6	6.3
X6	$[0, 0, +1, -1]$	4.3	4.9
U1	$[+1, -1, 0, 0]^{eu}$	5.6	5.9
U2	$[+1, 0, +1, 0]^{eu}$	6.4	7.6
U3	$[+1, 0, 0, +1]^{eu}$	7.5	8.3
U4	$[0, +1, +1, 0]^{eu}$	6.6	7.4
U5	$[0, +1, 0, +1]^{eu}$	6.8	7.3
U6	$[0, 0, +1, -1]^{eu}$	4.8	5.2

Table 1: *Relations between couplings $[\epsilon_{LL}, \epsilon_{LR}, \epsilon_{RL}, \epsilon_{RR}]$ for the compositeness models and the 95% C.L. limits on the compositeness scale, Λ, resulting from the ZEUS analysis of 1994-2007 $e^{\pm}p$ data. Each row of the table represents two scenarios corresponding to $\eta > 0$ (Λ^+) and $\eta < 0$ (Λ^-). The same coupling structure applies to d and u quarks, except for the models U1 to U6, for which the couplings for the d quarks are zero.*

ZEUS 1994-2007 (prel.) $e^{\pm}p$		
Model	Coupling Structure	95% C.L. (TeV) M_{LQ}/λ_{LQ}
$S_\circ^L$	$a_{LL}^{eu} = +\frac{1}{2}$	1.24
$S_\circ^R$	$a_{RR}^{eu} = +\frac{1}{2}$	1.02
$\tilde{S}_\circ^R$	$a_{RR}^{ed} = +\frac{1}{2}$	0.41
$S_{1/2}^L$	$a_{LR}^{eu} = -\frac{1}{2}$	0.94
$S_{1/2}^R$	$a_{RL}^{ed} = a_{RL}^{eu} = -\frac{1}{2}$	0.81
$\tilde{S}_{1/2}^L$	$a_{LR}^{ed} = -\frac{1}{2}$	0.60
S_1^L	$a_{LL}^{ed} = +1,\ a_{LL}^{eu} = +\frac{1}{2}$	0.87
$V_\circ^L$	$a_{LL}^{ed} = -1$	1.05
$V_\circ^R$	$a_{RR}^{ed} = -1$	0.77
$\tilde{V}_\circ^R$	$a_{RR}^{eu} = -1$	1.50
$V_{1/2}^L$	$a_{LR}^{ed} = +1$	0.50
$V_{1/2}^R$	$a_{RL}^{ed} = a_{RL}^{eu} = +1$	1.36
$\tilde{V}_{1/2}^L$	$a_{LR}^{eu} = +1$	1.60
V_1^L	$a_{LL}^{ed} = -1,\ a_{LL}^{eu} = -2$	1.88

Table 2: *Coefficients a_{ij}^{eq} defining the effective leptoquark couplings in the contact-interaction limit $M_{LQ} \gg \sqrt{s}$ and the 95% C.L. lower limits on the leptoquark mass to the Yukawa coupling ratio M_{LQ}/λ_{LQ} resulting from the CI analysis of the ZEUS 1994-2007 $e^{\pm}p$ data, for different models of scalar (upper part of the table) and vector (lower part) leptoquarks.*

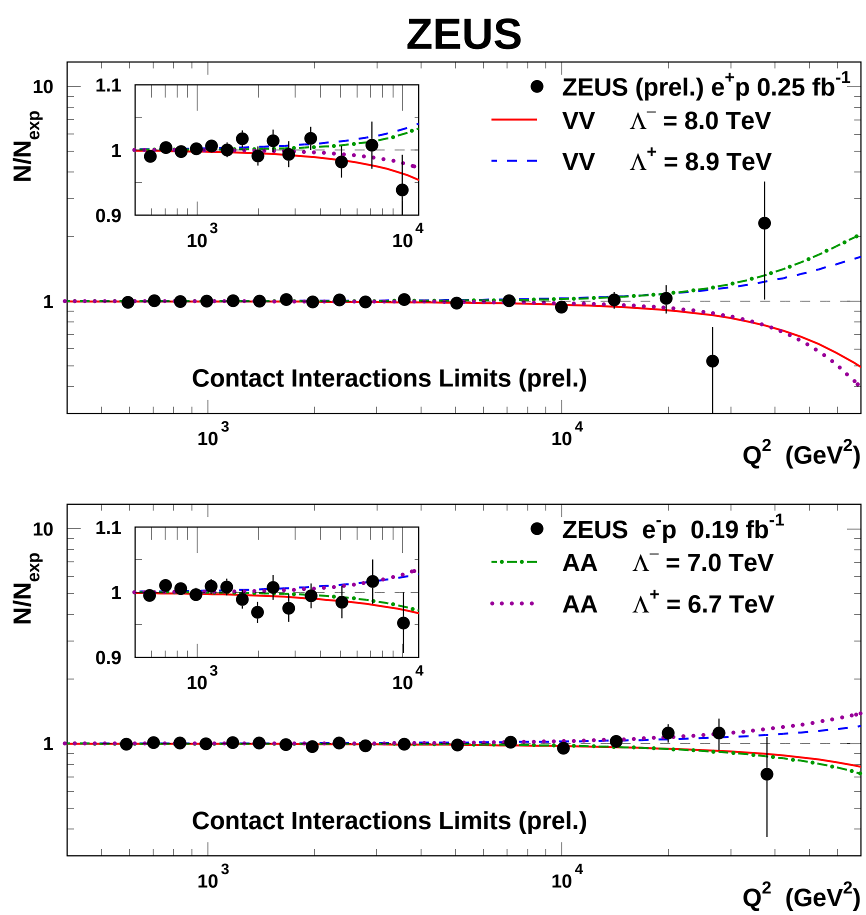

Figure 1: *ZEUS e^+p data (top plot) and e^-p data (bottom plot) compared with 95% C.L. exclusion limits for the effective mass scale in the VV and AA contact-interaction models, for positive (Λ^+) and negative (Λ^-) couplings (same four models are shown on both plots). Results are compared to the Standard Model expectations calculated using the CTEQ5D parton distributions. Model predictions are normalized to the data. The insets show the comparison in the $Q^2 < 10^4$ GeV^2 region, with a linear ordinate scale.*

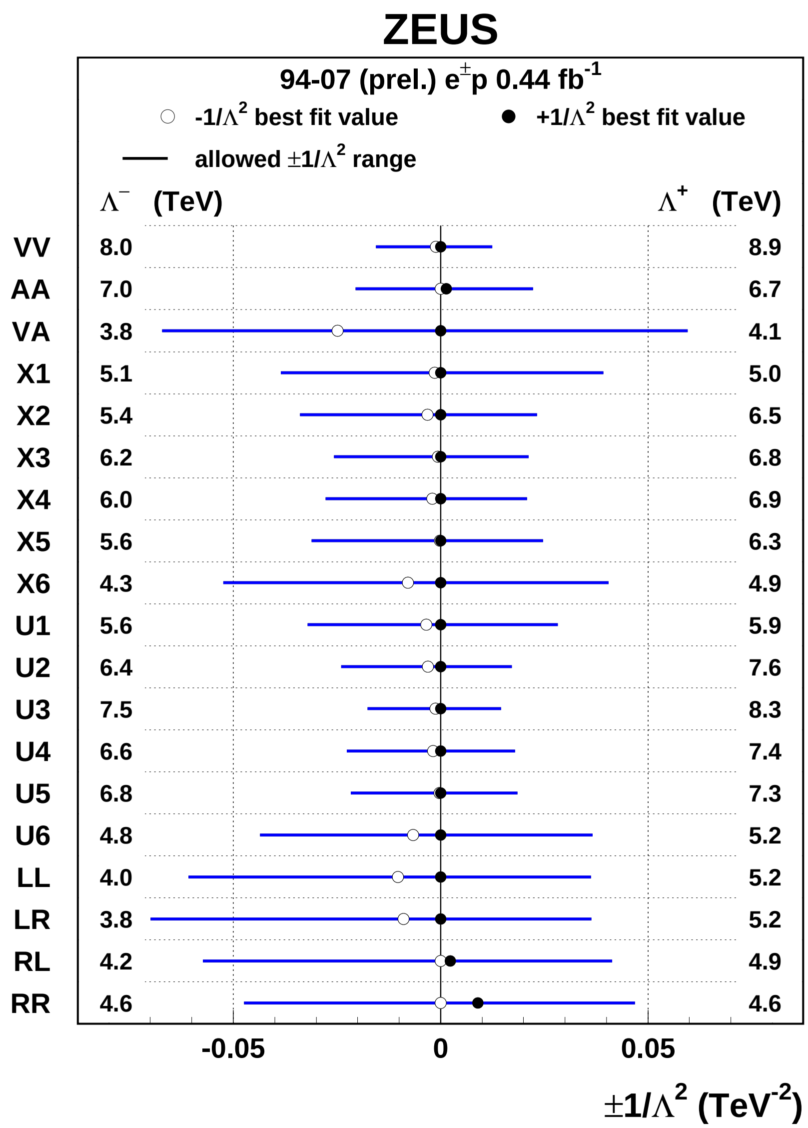

Figure 2: *Confidence intervals of $\pm 1/\Lambda^2$ at 95% C.L. for general CI scenarios studied in this paper (dark horizontal bars). The numbers at the right (left) margin are the corresponding lower limits on the mass scale Λ^+ (Λ^-). The filled (open) circles indicate the positions corresponding to the best-fit coupling values, for positive (negative) couplings.*

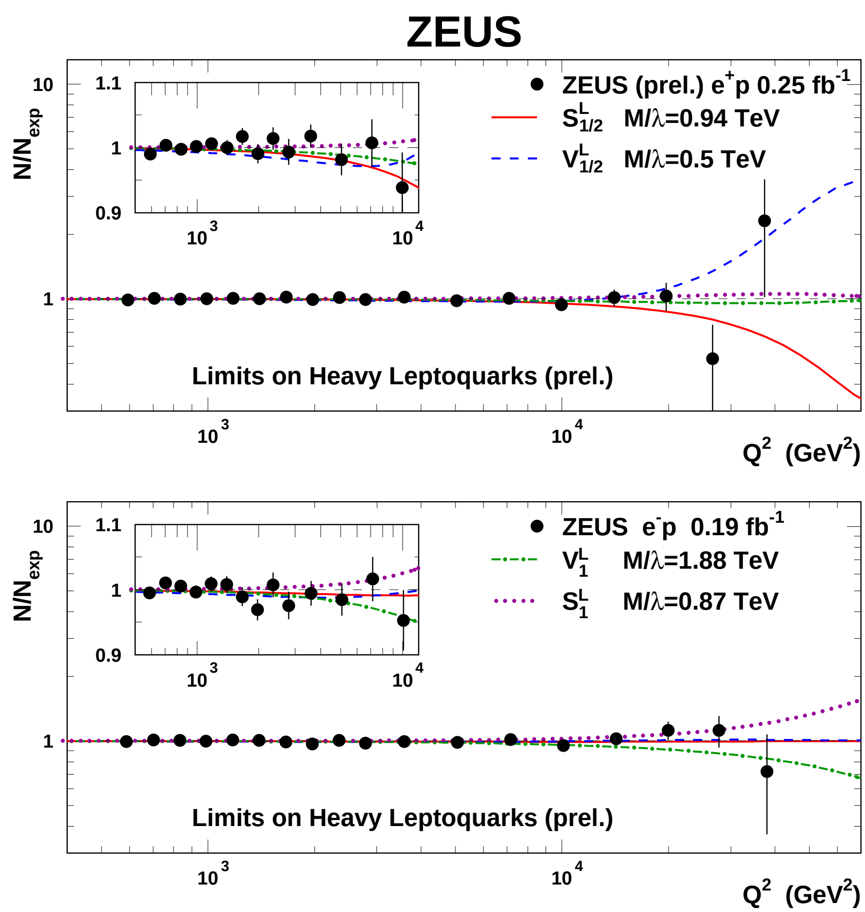

Figure 3: *ZEUS e^+p data (top plot) and e^-p data (bottom plot) compared with 95% C.L. exclusion limits for the ratio of the leptoquark mass to the Yukawa coupling, M/λ, for the $S^L_{1/2}$, S^L_1, V^L_1 and $V^L_{1/2}$ leptoquarks (same four models are shown on both plots). Results are compared to the Standard Model expectations calculated using the CTEQ5D parton distributions. Model predictions are normalized to the data. The insets show the comparison in the $Q^2 < 10^4$ GeV^2 region, with a linear ordinate scale.*

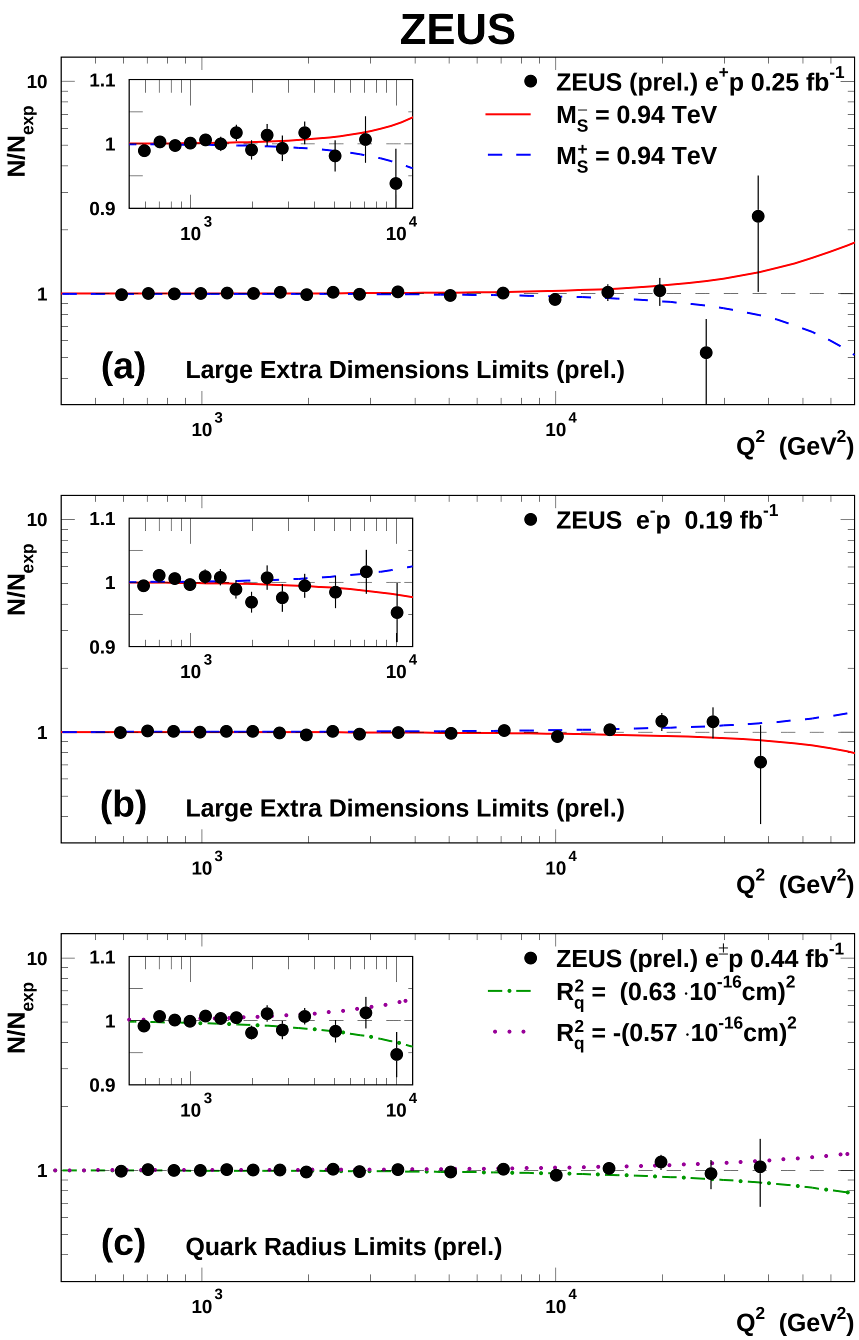

Figure 4: *ZEUS e^+p data (a) and e^-p data (b) compared with 95% C.L. exclusion limits for the effective Planck mass scale in models with large extra dimensions, for positive (M_S^+) and negative (M_S^-) couplings. (c) Combined 1994-2000 data compared with 95% C.L. exclusion limits for the effective mean-square radius of the electroweak charge of the quark. Results are compared to the Standard Model expectations calculated using the CTEQ5D parton distributions. Model predictions are normalized to the data. The insets show the comparison in the $Q^2 < 10^4$ GeV^2 region, with a linear ordinate scale.*